UDC 621.77.014
https://doi.org/10.17073/0021-3438-2024-3-73-86

Research article
Научная статья

Finite element simulation of hot cladding parameters for thin-sheet rolled products made of experimental Al–2%Cu–2%Mn alloy

A.N. Koshmin[1,2], **A.V. Zinoviev**[2], **S.O. Cherkasov**[2], **K.A. Tsydenov**[2]

[1] **Moscow Polytechnic University**
38 Bolshaya Semyonovskaya Str., Moscow 107023, Russia

[2] **National University of Science and Technology "MISIS"**
4 Bld. 1 Leninskiy Prosp., Moscow 119049, Russia

✉ Aleksander N. Koshmin (koshmin.an@misis.ru)

Abstract: An analysis was performed on the temperature, rate and force parameters of the hot cladding process for the experimental Al–2%Cu–2%Mn alloy with technically pure aluminum grade 1050A, as well as on the stress-strain state of the metal in the deformation zone at reductions of 30, 40, and 50 %. Plastometric tests were conducted within the temperature range of 350–450 °C, strain rates of 0.1–20 s^{-1}, and true strain of 0.1–0.9, and coefficients for calculating the flow stress of the experimental alloy were determined. The thermal conductivity of the Al–2%Cu–2%Mn alloy under hot deformation conditions at temperatures of 350, 400, and 450 °C was theoretically calculated to be 161, 159, and 151 W/(m·K), respectively. The study of the cladding process on a two-high rolling mill was carried out using the QForm finite element simulation software. It was found that when the metal of the cladding layer comes into contact with the roll, its temperature decreases by approximately 100 °C, with the temperature across the height of the composite equalizing within 20–30 ms after exiting the deformation zone. The rolling force is evenly distributed between the two rolls in all cases considered, while the rolling torque on the roll on the cladding layer side is half that on the roll contacting the base layer, which is characteristic of asymmetric rolling. Points characterized by optimal bonding conditions of the rolled layers were identified, located at 10 % and 70 % of the deformation zone length along the rolling axis, where normal stresses significantly prevail over shear stresses. It was determined that the formation of these areas is due to the nature of plastic flow, including the presence of a non-deforming hard layer and a sticking zone.

Keywords: finite element simulation, hot rolling, cladding, aluminum alloy, rheology, plastic deformation, deformation zone (DZ).

Acknowledgments: The study was carried out with the financial support of the Russian Science Foundation grant Project No. 23-79-01172, https://rscf.ru/project/23-79-01172/

For citation: Koshmin A.N., Zinoviev A.V., Cherkasov S.O., Tsydenov K.A. Finite element simulation of hot cladding parameters for thin-sheet rolled products made of experimental Al–2%Cu–2%Mn alloy. *Izvestiya. Non-Ferrous Metallurgy.* 2024;30(3):73–86.
https://doi.org/10.17073/0021-3438-2024-3-73-86

Конечно-элементное моделирование параметров горячего плакирования тонколистового проката из экспериментального сплава Al–2%Cu–2%Mn

А.Н. Кошмин[1,2], **А.В. Зиновьев**[2], **С.О. Черкасов**[2], **К.А. Цыденов**[2]

[1] **Московский политехнический университет**
Россия, 107023, г. Москва, ул. Большая Семеновская, 38

[2] **Национальный исследовательский технологический университет «МИСИС»**
Россия, 119049, г. Москва, Ленинский пр-т, 4, стр. 1

✉ Александр Николаевич Кошмин (koshmin.an@misis.ru)

Аннотация: Выполнен анализ температурных, скоростных и силовых параметров процесса горячего плакирования экспериментального сплава Al–2%Cu–2%Mn технически чистым алюминием марки 1050А, а также напряженно-деформированного состояния металла в очаге деформации при относительной деформации 30, 40 и 50 %. В интервалах температур 350–450 °С, скоростей деформации 0,1–20 $с^{-1}$ и истинной деформации 0,1–0,9, проведены пластометрические испытания и определены коэффициенты для расчета сопротивления деформации экспериментального сплава. Расчетно-теоретически определена теплопроводность сплава Al–2%Cu–2%Mn для условий горячего деформирования при температурах 350, 400 и 450 °С, которая составила 161, 159 и 151 Вт/(м·К) соответственно. Изучение особенностей процесса плакирования на двухвалковом стане выполнено в комплексе конечно-элементного моделирования QForm. Установлено, что при контакте металла плакирующего слоя с валком происходит его охлаждение на ~100 °С, а выравнивание температуры по высоте композита – в течение 20–30 мс после его выхода из очага деформации. Усилие прокатки равномерно распределено между двумя валками во всех рассматриваемых случаях, а момент прокатки на валке со стороны плакирующего слоя в 2 раза ниже, чем на контактирующем с основным, что характерно для асимметричной прокатки. Определены точки, характеризуемые оптимальными условиями соединения слоев проката, расположенные на расстоянии 10 % и 70 % по длине очага деформации вдоль оси прокатки, в которых нормальные напряжения существенно превалируют над касательными. Установлено, что возникновение данных областей обусловлено характером пластического течения, в том числе наличием зоны отсутствия деформации твердого слоя и зоны прилипания.

Ключевые слова: конечно-элементное моделирование, горячая прокатка, плакирование, алюминиевый сплав, реология, пластическая деформация, очаг деформации (ОД).

Благодарности: Исследование выполнено за счет гранта Российского научного фонда № 23-79-01172, https://rscf.ru/project/23-79-01172/

Для цитирования: Кошмин А.Н., Зиновьев А.В., Черкасов С.О., Цыденов К.А. Конечно-элементное моделирование параметров горячего плакирования тонколистового проката из экспериментального сплава Al–2%Cu–2%Mn. *Известия вузов. Цветная металлургия*. 2024;30(3):73–86. https://doi.org/10.17073/0021-3438-2024-3-73-86

Introduction

Aluminum-based alloys have found widespread use in various industries due to the advantageous combination of their operational characteristics and relatively low cost [1]. The most common group consists of heat-treatable alloys in the Al—Cu system (1201, D16, D20, etc.). However, a common drawback of materials in this group is the necessity of thermal processing — such as homogenization of ingots before deformation, quenching, and prolonged artificial aging of deformed semi-finished products (18—36 hours) — to achieve the maximum possible strength, which significantly complicates the manufacturing process of these semi-finished products.

In [2], a new deformable and non-heat-treatable Al—2%Cu—2%Mn alloy, economically alloyed with Zr and Sc, was studied. It was found to exhibit better manufacturability compared to its Al—Cu system counterparts. The research [3] indicates that even without additional alloying, the base experimental alloy demonstrates a good level of functional properties at room

temperature and retains them when the temperature increases during operation.

It is known that aluminum alloys alloyed with copper are susceptible to stress corrosion cracking and exfoliation corrosion [4]. Therefore, various surface modification techniques are used to protect products made from these alloys [5]. Among them, cladding aluminum alloys with technical aluminum by roll bonding is the most straightforward to implement and, unlike other methods, provides reliable protection of the base layer under conditions of intense thermal and mechanical stresses [6].

Despite the rather long history of practical use of the hot cladding process for high-strength aluminum alloys and the large number of research works conducted, including those using finite element (FE) analysis [7; 8], the mechanisms of bonding dissimilar metals have not been fully established. Several theories explain the creation of a strong adhesive bond between metals as a result of pressure processing: the "film" theory, diffusion theory, and complex theory [9]. However, it is indisputable that the primary process determining metal bonding is joint plastic deformation. This process is characterized by the duration of exposure, the magnitude of the generated stresses, the value and rate of deformation, and the temperature conditions of the process [10; 11]. However, to date, there are no studies examining this problem in terms of the influence of the geometric parameters of the deformation zone (DZ), the force, and the speed conditions of deformation of layered flat rolled products on the bonding process.

The objectives of this study were to investigate the plastic characteristics of the Al—2%Cu—2%Mn alloy, develop and construct a finite element model for its cladding with technically pure aluminum under various deformation parameters, and analyze the results obtained.

Characteristics of research materials

The materials used for the workpieces were technically pure aluminum grade 1050A (EN 573-3:2007) and an experimental Al—2%Cu—2%Mn alloy (hereafter referred to as 2Cu2Mn). Their chemical composition is presented in Table 1. To obtain the physical and mechanical properties necessary for simulation, a billet of the 2Cu2Mn alloy measuring 20×120×135 mm was cast and then rolled at a temperature of 400 °C on a two-high rolling mill DUO210X300 at a roll circumferential speed of 30 rpm to a thickness of 15 mm to produce a deformed structure. Cylindrical samples with a diameter of 5 mm and a length of 10 mm were taken from the rolled sheet along the deformation direction. The rheology of these samples was studied using a quenching-deformation dilatometer DIL805A/D (TA Instruments, USA). The temperature and strain rate parameters of the dilatometer tests were selected based on the conditions characteristic of hot deformation for this material and included tests at temperatures (t) of 350, 400, 450 °C and strain rates ($\bar{\varepsilon}$) of 0.1, 1.0, 10, and 20 s^{-1}. The samples were tested by compression until a true strain value of $\varepsilon_t = 0.9$. As a result, deformation curves of the experimental alloy were obtained, from which, after adjusting for friction and temperature, the coefficients for the equation calculating the flow stress (σ) considering thermal softening were determined [12]:

$$\sigma = e^{A}\bar{\varepsilon}^{m}\varepsilon_t^{n_1}e^{\varepsilon_t n_2}e^{tl},$$

where A, m, n_1, n_2, l are coefficients characterizing the material properties.

The calculated values of the coefficients for the experimental and standard [13] alloys are given in Table 2. The table also presents the calculated correlation coefficient (R^2) and the Fisher criterion (F), confirming the adequacy of the alloy strengthening models.

A necessary parameter for the modeling of the experimental alloy is its thermal conductivity, which was calculated based on the Wiedemann—Franz law:

$$k/\gamma = LT,$$

where k is the thermal conductivity in W/(m·K); γ is the electrical conductivity in S/m; L is the Lorentz number, equal to $2.23\cdot10^{-8}$ W·Ω·K^{-2} for aluminum alloys [13]; T is the temperature in K.

Table 1. **Chemical composition of the alloys under investigation**

Таблица 1. Химический состав исследуемых сплавов

Alloy	Composition, wt.%				
	Al	Cu	Mn	Si	Fe
2Cu2Mn	Base	1.93 ± 0.05	1.94 ± 0.04	0.05 ± 0.04	≤ 0.01
1050A	99.79	–	–	0.18 ± 0.03	0.03 ± 0.02

Table 2. **Coefficients for flow stress calculation in hot rolling processes**

Таблица 2. Коэффициенты для расчета сопротивления деформации при горячей прокатке

Alloy	A	m	n_1	n_2	l	R^2	F
2Cu2Mn	6.2121	0.0756	–0.0382	–0.0046	–0.0616	0.9678	0.0170
1050A	4.9577	0.1475	0.1607	–0.0035	–0.0174	0.9744	0.0165

The specific electrical conductivity of a sample of the 2Cu2Mn alloy, taken from the hot-deformed sheet, was measured at room temperature using an eddy current structural analyzer VE-26NP (Russia) and was found to be $15{,}3 \cdot 10^6$ S/m. The value of γ for the experimental alloy at elevated temperatures was obtained by extrapolating known data [14] to the measured value. Thus, the calculated thermal conductivity of the alloy at temperatures of 350, 400, and 450 °C was 161, 159, and 151 W/(m·K), respectively. The thermal conductivity and specific heat capacity values for the cladding layer material were taken from the standard material library of the modeling software for the 1050A alloy and were 226 W/(m·K) and 930 J/(kg·K), respectively [15].

Finite element simulation methodology

Geometric parameters of the model and initial data

The hot rolling — cladding process was simulated in a plane strain mode using the QForm 10.3 software package [16]. The geometry of the tool, along with parameters and characteristics similar to those of the DUO210X300 rolling mill (Russia), was imported into the modeling program (Fig. 1, *a*). The workpieces used were two plates made from the studied alloys with different initial thicknesses h_b and h_c. The layered workpiece was then deformed with a reduction ε of 30 %, 40 %, and 50 %, so that the values of h_b and h_c in each case were 5.85 and 0.65 mm, 6.3 and 0.7 mm, and 6.75 and

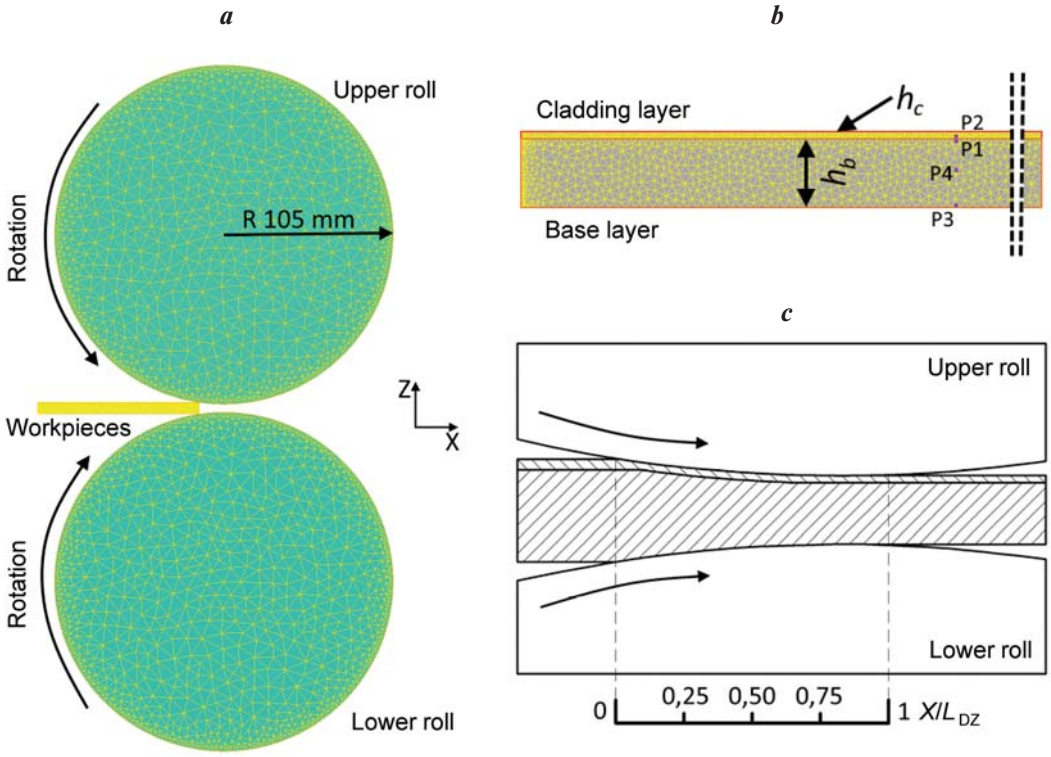

Fig. 1. The geometry of the roll unit (***a***), workpieces (***b***), and deformation center (***c***)

Рис. 1. Геометрия валкового узла (***a***), заготовок (***b***) и очага деформации (***c***)

0.75 mm, respectively. As a result, the final total thickness of the clad sheet was 5 mm. The initial length and the non-represented width in the plane strain model were each 100 mm.

Traced points, located through the thickness of the workpiece at key and particularly indicative sections, were used to study the contact stresses and flow velocities. According to Fig. 1, *b*, these points are located as follows:

— at the contact between the base layer (P1) and the cladding layer (P2);

— at the point of contact between the base layer and the lower roll (P3);

— in the middle of the total thickness of the rolled product (P4).

The primary work of consolidating the layers occurs directly due to the stresses within the deformation zone. Fig. 1, *c* shows a view of the deformation zone, where the length of the contact arc between the metal and the roll relative to the *X*-axis (X/L_{DZ}) is schematically indicated. The analysis of the modeling data and the construction of graphs were performed concerning this section.

The model used triangular-shaped finite elements (FE), which are well-suited for simulating plane strain rolling processes. To increase the calculation accuracy, an adaptive mesh refinement was chosen, with a mesh adaptation coefficient of 3 in the workpieces. This means that the ratio of the maximum size of the modeled object to the size of any finite element in the mesh will be maintained within a specified range, which is beneficial when using workpieces of different initial thicknesses and when they are thinned during rolling. The main initial parameters of the model are presented below:

Material of the rolls 41Cr4

Roll temperature, °C..... 25

Workpiece temperature, °C..... 400

Ambient temperature, °C..... 25

FE number in the tool, thousand units 2.5

FE number in the workpiece
at the beginning/end of modeling,
thousand units.....10/15

Time step, ms 2.5

Deformation and thermal models

The coordinate system was chosen so that the axis of the least deformation coincided with the missing axis

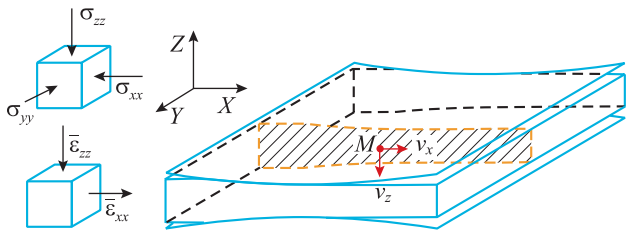

Fig. 2. Plane strain state in the case of thin sheet rolling

Рис. 2. Плоское деформированное состояние в случае прокатки тонкого листа

in the coordinate system. In the case of flat rolling, this direction can be considered the *Y*-axis (Fig. 2), as it is in this direction that only the widening of the metal occurs, which is significantly less than the reduction and elongation. In this case, the mesh elements move only in the directions of v_x and v_z, here are no shear stresses on the planes perpendicular to the *Y*-axis, and the normal stress in the *Y*-axis direction depends on the normal stresses along the other axes and during plastic deformation is equal to:

$$\sigma_{yy} = \frac{1}{2(\sigma_{xx} + \sigma_{zz})}.$$

Stress tensors (T_σ) and final strains (T_E) in the case under consideration are as follows:

$$T_\sigma = \begin{pmatrix} \sigma_{xx} & 0 & \sigma_{xz} \\ 0 & \sigma_{yy} & 0 \\ \sigma_{zx} & 0 & \sigma_{zz} \end{pmatrix}, \quad T_E = \begin{pmatrix} E_{xx} & 0 & E_{xz} \\ 0 & 0 & 0 \\ E_{zx} & 0 & E_{zz} \end{pmatrix}.$$

The equivalent (plastic) strain (ε_{eq}) was calculated using the equivalent plastic strain rate ($\bar{\varepsilon}_{eq}$) by integrating the sum of the increments along the particle's trajectory:

$$\varepsilon_{eq} = \int_t \bar{\varepsilon}_{eq} dt,$$

$$\bar{\varepsilon}_{eq} = \sqrt{\frac{4}{9}\left\{\frac{1}{2}[(\bar{\varepsilon}_{xx} - \bar{\varepsilon}_{zz})^2 + \bar{\varepsilon}_{xx}^2 + \bar{\varepsilon}_{zz}^2] + \frac{3}{4}\bar{\gamma}_{xz}^2\right\}}.$$

A "simple" heat exchange mode was applied for calculating the heat transfer between the pairs of workpiece—workpiece and workpiece—tool, which limited the movement of heat flow from one object to another by a near-surface layer with a thickness of 5 linear mesh elements. This mode was chosen due to the high speed of the rolling process and, consequently, the short contact time between the workpieces and the tool, measured in

milliseconds. The propagation of the heat flow (q_n) in this case is normal in nature. Its magnitude is calculated by the equation:

$$q_n = b\alpha(t_1 - t_2),$$

where t_1 and t_2 are the temperatures of the model objects, °C; α is the heat transfer coefficient; $b = 0.05$ is a pause coefficient that accounts for the distance between the objects. The heat transfer coefficient values between the tool and the workpieces, as well as between the layers of the workpiece, were assumed to be 100000 and 120000 W/(m^2·K), respectively [17].

Contact model

The contact model of objects in the simulation of the cladding process is a crucial factor that influences the overall adequacy of the model. The Siebel law was used to describe the contact interaction between the workpiece—workpiece and workpiece—tool pairs, which defines the shear stress (τ) on the surface of the workpiece as the product of the friction factor (k_f) and the flow stress in the layers of the workpieces that are in contact with the tool and with each other (σ):

$$\tau = k_f \frac{\sigma}{\sqrt{3}}.$$

The friction factor was determined experimentally by measuring the duration of the rolling process for standard samples with a length of 200 mm made from alloys similar to those being studied and comparing this time with the modeled one. The friction factor for the workpiece—tool pairs, including at the roll—cladding layer and roll—base layer boundaries, was assumed to be 2.5, and for the workpiece—workpiece pair, it was 4. A higher friction factor between the workpieces was chosen based on the preparation of their surfaces in contact with each other by degreasing and mechanical processing (increasing roughness).

In QForm, a special contact element is used for the numerical implementation of the joint deformation of two modeled objects (workpieces) since the nodes of the finite element mesh in the contacting bodies do not generally coincide. Figure 3 schematically shows the principle of this interaction. For clarity, the contacting elements are separated along the normal by a distance comparable to the size of the element. The direction of the normal is indicated by the vector $\vec{n}$. The nodal velocities (v_p) are used as the nodal unknowns. In this case, the normal force function P_n, which ensures the minimization of penetration along

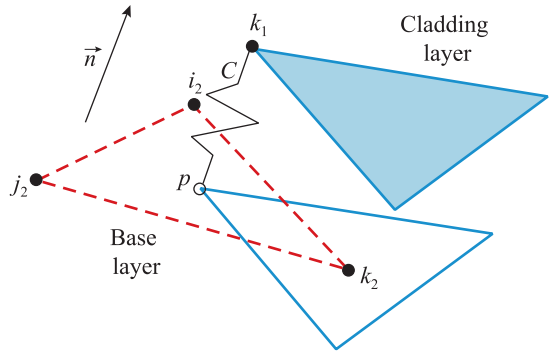

Fig. 3. Schematic of contacting finite elements of two workpieces [17]

Рис. 3. Схема контактирующих конечных элементов двух заготовок [17]

the normal to the contact surfaces of the workpieces, is as follows:

$$P_n = C(v_n^{k_1} - v_n^p).$$

where C is a penalty coefficient determined as a value that exceeds the largest of the diagonal coefficients of the stiffness matrices of the two contacting bodies. Thus, using shape functions, the forces at the nodes of the contact element are determined by the formula:

$$P_n = P_n^{k_1} - P_n^{i_2} - P_n^{j_2} - P_n^{k_2}.$$

Results and discussion

Temperature and force parameters of the cladding process

Regardless of the degree of deformation ε, the formation of temperature fields in the workpiece follows a similar pattern (Fig. 4). At the entry into the deformation zone (DZ), there is an almost instantaneous drop in the metal temperature at the contact with the tool — on average by 100 °C. As the workpieces move along the rolling axis, their surface temperatures gradually equalize, tending toward the temperature of the internal non-contact area. This is facilitated by the deformation heating of the base layer, which not only does not decrease but even increases its temperature by 10 °C from the initial value.

The cooling of the cladding layer deserves special attention. The drop in its temperature upon contact with the roll occurs throughout its thickness but does not spread to the base layer, whose temperature remains high. This fact is due to the peculiarities of the software calculation of heat transfer, which is conducted sepa-

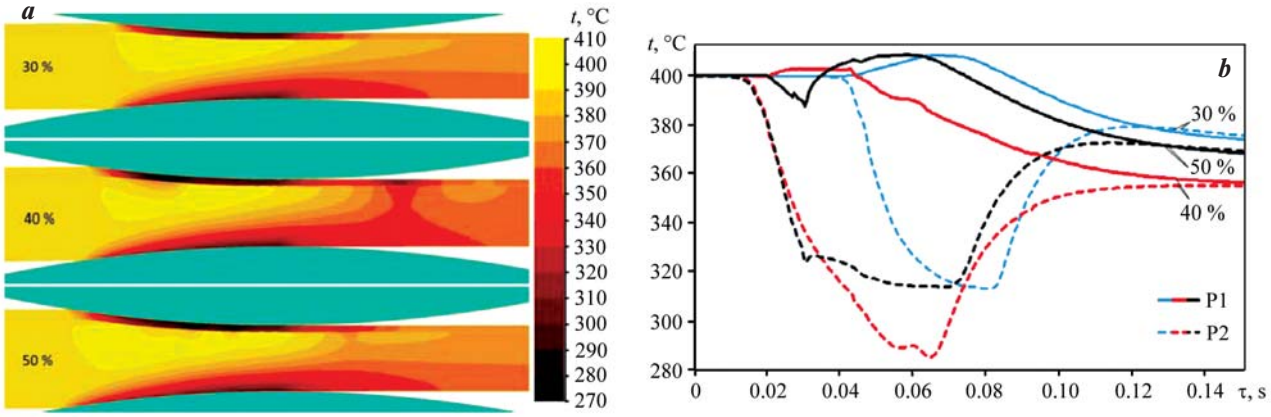

Fig. 4. Temperature fields in the deformation zone (***a***) and temperature as a function of deformation zone transit time in the base (P1) and cladding (P2) layers during rolling (***b***)

Numbers at the curves are values of the strain ratio

Рис. 4. Температурные поля в очаге деформации (***a***) и температура в зависимости от времени прохождения очага деформации в основном (P1) и плакирующем (P2) слоях в процессе прокатки (***b***)

Цифры у кривых – значения степени относительной деформации

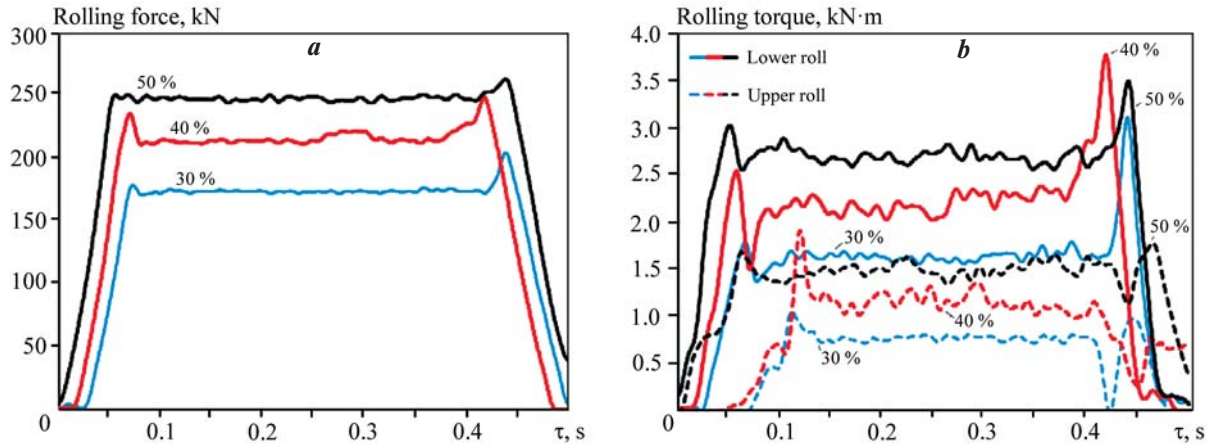

Fig. 5. Change in force (***a***) and torque (***b***) during the rolling process

Numbers at the curves are values of the strain ratio

Рис. 5. Изменение усилия (***a***) и момента (***b***) в ходе прокатки

Цифры у кривых – значения степени относительной деформации

rately for each workpiece without the possibility to exclude the consideration of the pause coefficient *b* after passing through the deformation zone. In other words, this temperature model does not account for the formation of a welded joint (adhesion) between the layers. Nevertheless, the results of the temperature changes in the layered rolled product appear adequate. The temperature of each layer in the contact areas tends to equalize within 20—30 ms after the composite exits the deformation zone.

The change in the force parameters of the cladding process follows a fairly traditional pattern. The rolling force change curves (Fig. 5) clearly show all the main stages of the process: the capture of the workpieces by the rolls, the steady stage, and the exit of the metal from the rolls. The force value at the steady stage is 175, 215, and 250 kN for reductions ε of 30 %, 40 %, and 50 %, respectively. Here, there is a trend of increasing rolling force by 20 % with a 10 % increase in reduction. The rolling torque varies less predictably over time. Peaks corresponding to the capture and exit of the metal from the rolls are also observed here, but the steady stage is characterized by numerous oscillations. This may be due to the presence of two objects in the deformation zone, whose interfacial friction is uneven along the DZ.

Another feature is the difference in the rolling torque acting on the upper and lower rolls. The torque on the lower roll, which is in contact with the metal of the base layer, is on average twice as high as that on the upper roll in all cases considered. This is due to the difference in the flow stress of the investigated alloys, which directly affects the conditions of contact friction. However, when comparing the rolling forces acting on the lower and upper rolls in each simulation case, such a high discrepancy was not observed, with a maximum difference of 10 %.

Stress-strain state of the rolled product in the deformation zone

The nature of the formation of equivalent strain (ε_{eq}) and the distribution of the equivalent plastic strain rate ($\bar{\varepsilon}_{eq}$) along the deformation zone (DZ) is shown in Fig. 6. As can be seen, the degree of relative reduction significantly influences these characteristics. As the reduction increases, the extent of the deformation zone noticeably expands, and consequently, the contact time of the joined surfaces under pressure also increases. The work hardening of the base layer occurs less intensively with increasing ε compared to the cladding layer. This is due to both the temperature conditions (significant cooling throughout the thickness of the cladding layer) and the different patterns of equivalent strain rate distribution, which in the contact zone of the cladding layer was 0.9, 1.25, and 1.6 for relative reductions of 30 %, 40 %, and 50 %, respectively. The values of the equivalent strain rate are roughly the same in all cases: up to 80 s^{-1} at the entry to the DZ (in the zone of maximum compression) and an average of 15 s^{-1} in the middle of the thickness of the rolled product (and on average throughout the entire DZ).

The distribution fields $\bar{\varepsilon}_{eq}$ also allow for some observations. Deformation is most intense at the entry and exit from the deformation zone in the areas where the workpieces contact the tool. The extent of these zones differs in each case, but their volumetric share relative to the entire geometric DZ is the same. The occurrence of such distinct X-shaped patterns in the distribution $\bar{\varepsilon}_{eq}$ is associated with the nature of metal flow and the accompanying development of shear deformations in these areas.

Several studies [18; 19] assert the existence of a pattern of adhesion in layered rolled products with significantly different strengths (hardness). They suggest that a high difference in the strength of the contact surfaces of the joined sheets promotes uneven metal flow of the workpieces within the deformation zone relative to each other. This creates additional shear stresses between the layers, reducing the effect of normal stresses and, as a result, hindering the formation of a strong welded joint in the DZ. Also, considering the "film" theory of metal bonding, it can be assumed that the high strength of the surfaces of the joined sheets will contribute to more effective oxide film destruction during deformation and the bonding of the formed juvenile areas.

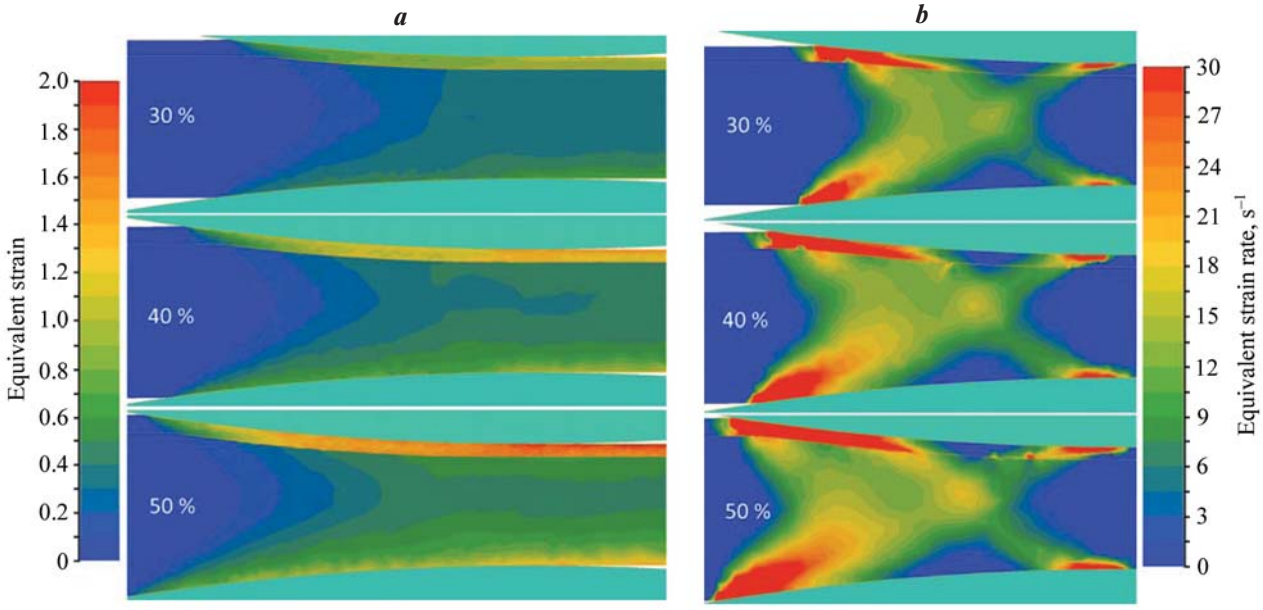

Fig. 6. Distribution fields of equivalent strain (***a***) and strain rate (***b***) in the deformation zone at different values of strain

Рис. 6. Поля распределения эквивалентной деформации (***a***) и скорости деформации (***b***) в ОД при разных значениях относительного обжатия

Figure 7 shows the change in flow stress (σ) of the base (P1) and cladding (P2) layers along the deformation zone. Flow stress in QForm is calculated as the distribution of σ (flow stress) values, set in the material properties, depending on the equivalent strain, strain rate, and temperature. It should be noted that the length of the DZ relative to the *X*-axis is standardized for all cases considered, but its actual geometric length, as well as the contact time under rolling force, increases by ~15 % with each 10 % increase in reduction. The graphs show that the flow stress of the base layer changes little with varying reduction and averages 100 MPa, while for the cladding layer, it is more affected by reduction: ~70 MPa at ε = 30 and ~80 MPa at ε = 40 and 50 %.

The increase in σ is due to the regular growth of ε_{eq} with increasing reduction, and the equal σ values at ε = 40 and 50 % can be explained by the greater cooling of the cladding layer at ε = 40, as clearly shown in Fig. 4. In all cases considered, at the length of the defor-

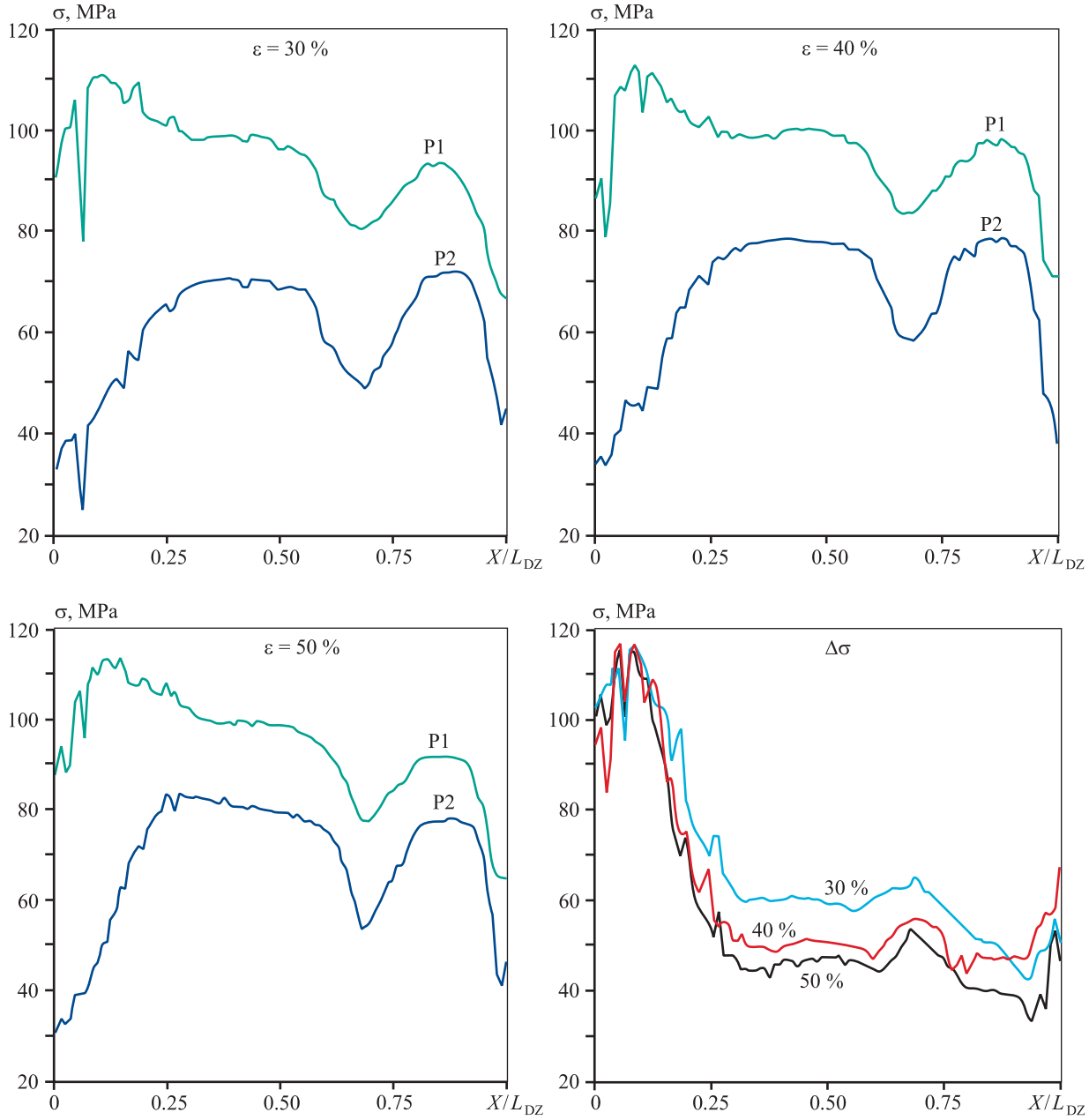

Fig. 7. Change in the flow stress of the base (P1) and cladding (P2) layers and the difference in their flow stresses (Δσ) along the length of the deformation zone

Рис. 7. Изменение сопротивления деформации основного (P1) и плакирующего (P2) слоев и разность их сопротивления деформации (Δσ) вдоль длины очага деформации

mation zone of 0.65—0.70, a decrease in σ values of approximately 25 % can be observed, followed by their recovery to the previous level, which is maintained until the metal exits the rolls. This fact is explained by the passage of the traced points through an area with relatively low equivalent plastic strain rate (blue areas in Fig. 6, *b*), as well as a general reduction in the normal and shear stresses (σ_{xx} and σ_{zz}, respectively) acting in this section. Comparing the difference in flow stress values for each layer's surface (Δσ), a systematic decrease with increasing relative strain is noted, which is evident: the smallest Δσ value is achieved at a 50 % reduction. These graphs also indicate that the achievement of surface layer strength uniformity is ensured by the strengthening of the cladding layer on one side and the softening of the base layer due to heating on the other.

The combination of rolling process parameters that occur during the joint deformation of two workpieces, characterized by inhomogeneity along the length and height of the deformation zone (DZ), such as temperature, flow velocity, strain rate, surface strength of the layers, and others, leads to an increase in the shear stresses acting at the layer interfaces. To assess their influence on the formation of the composite bond, standard QForm subroutines — "Pressure" and "Friction" — were used to calculate the values of normal contact pressure (σ_p) and shear friction stress (τ_f).

Figure 8, *a* shows the change in shear stress along the deformation center. It is evident that the value of τ_f at each point of the DZ and in each case considered may differ from the presented one due to being subject to many poorly controlled factors of contact interaction between the two workpieces during joint deformation. Nonetheless, the nature of the obtained stress distribution patterns along the DZ remains consistent with rolling at different ε values. For example, it can be noted that τ_f remains almost unchanged from the moment the metal enters the deformation center until it reaches 0.1 of the DZ length, which is associated with the absence of plastic deformation in the base layer in this section. Then, as it progresses along the DZ, the inhomogeneity of strain rates and plastic flow in the layers increases, leading to a rise in τ_f. Approaching the neutral section of the DZ, the stress level gradually decreases toward zero, only to rise again afterward.

The nature of the normal stress variation along the deformation zone is more uniform. It fluctuates from 150 MPa at the entry to the DZ to 225 MPa at the exit. This is also reflected in the graph of the σ_p/τ_f (Fig. 8, *b*). As seen from the curves, this ratio is 5 for more than 70 % of the DZ length, indicating generally favorable conditions for the formation of an interlayer bond. In each case considered, two characteristic peaks can be noted on the curves — at 0.1 and 0.7 of the DZ length. The first peak symbolizes the onset of the welded bond formation between the layers, associated with the beginning of plastic deformation in the base layer, while the second is linked to improved contact interaction conditions in this section, specifically the drop in strain rate and the accompanying reduction of τ_f to zero. It can be assumed that in this point, the most significant bonding work between the layers occurs under the influence of normal stresses.

Discussion of modeling results

Figure 9 shows the change in the velocity of traced points located at the roll contact, at the interlayer

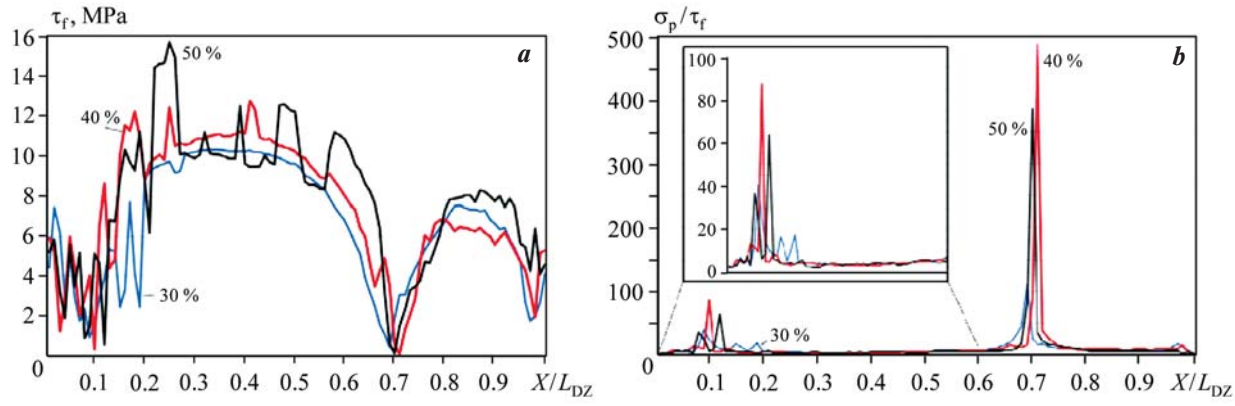

Fig. 8. Variation along the deformation zone of tangential stresses between rolled layers (***a***) and the ratio of normal stress to tangential stress (***b***)

Рис. 8. Изменение вдоль очага деформации касательных напряжений между слоями проката (***a***) и отношения нормального напряжения к касательному (***b***)

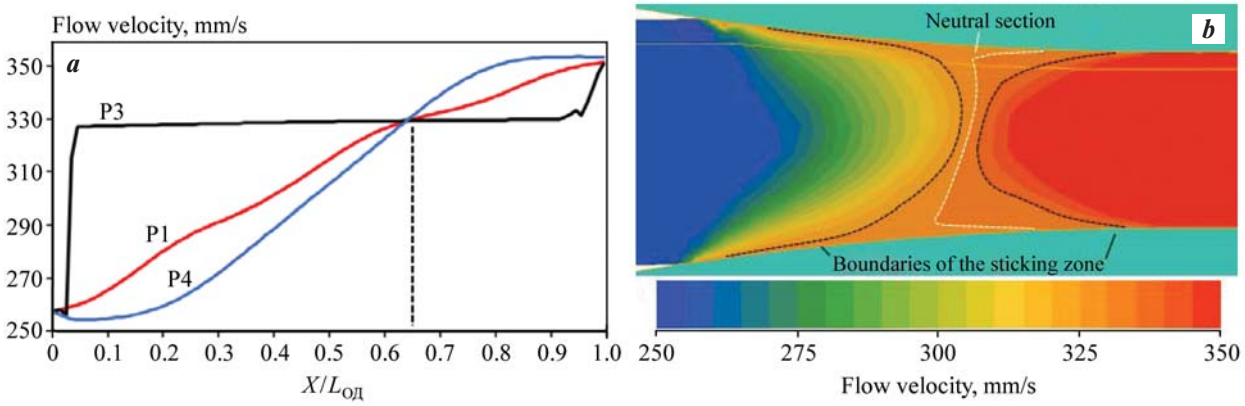

Fig. 9. Velocity of traced points along the *X*-axis (***a***) and flow velocity fields in the deformation zone (***b***)

Рис. 9. Скорость движения трассируемых точек вдоль оси *X* (***a***) и поля скорости течения в очаге деформации (***b***)

boundary, and at half the thickness of the composite during rolling with ε = 40 %. The curves represent a typical pattern for the longitudinal rolling process, allowing for the delineation of lagging and leading zones, positioned at 0.65 of the deformation zone length. At the same time, the sharp changes in values observed in Figs. 7 and 8 manifest themselves at a deformation zone length of 0.70. This is explained by the significant inhomogeneity in the distribution of metal flow velocity along the height of the deformation zone, as seen in the fields of the workpiece in Fig. 9. It can be noted that the sticking zone has an *I*-shaped form, and its center (neutral section) is slightly tilted, which is due to the rolling of dissimilar metals and, consequently, different torque values on the upper and lower rolls.

Thus, the nature of the plastic flow of metal in the deformation zone had the most significant influence on the results presented in the previous section. Under its influence, zones with low strain rate values were formed, which contributed to the reduction of flow stress in both layers. In this same area, the shear stresses are equal to zero.

The results obtained from the cladding modeling at different degrees of reduction are ambiguous. On one hand, increasing the degree of deformation has strengthened the cladding layer, thereby significantly reducing the ratio of the flow stress of the base layer to the cladding layer (σ_{p1}/σ_{p2}) from 3 to 1.5. On the other hand, the influence of the degree of deformation had little effect on the friction stresses acting along the rolling axis. This suggests that the influence of contact and interlayer friction under thin sheet rolling conditions is insignificant, and the success of metal layer bonding in this case is ensured by the action of normal stresses, which are enhanced by increasing the degree of deformation.

Overall, the comparison of the results obtained in this study with elements of the classical theory of longitudinal rolling [20—23] and modern computational and experimental results [24—29] allows us to conclude the adequacy of the developed model and the effectiveness of the applied computational methods and software package.

Conclusion

1. Using the QForm finite element simulation software, the cladding process of the experimental Al—2%Cu—2%Mn alloy with technically pure aluminum was simulated at reduction ratio of 30 %, 40 %, and 50 %. The temperature-rate and deformation parameters of the process, as well as the metal stresses in the layers along the deformation zone, were studied.

2. It was found that the strengthening of the cladding (softer) layer occurs more intensively with increasing deformation degree. The equivalent strain in the contact zone of the cladding layer with the base layer at relative reductions of 30 %, 40 %, and 50 % was 0.9, 1.25, and 1.6, respectively. This fact contributed to the reduction of the difference in flow stress between the contact surfaces of the rolled layers.

3. When studying the features of contact interaction between the surfaces of the layered rolled product, characteristic areas were identified along the length of the deformation zone at 0.1 and 0.7 relative to the *X*-axis, which are characterized by the dominance of normal stresses over shear stresses. The formation of these areas was facilitated by uneven metal flow in the deformation zone, caused by the difference in the deformation characteristics of the base and cladding layer materials.

4. The calculated values of normal and shear stresses between the layers of the workpieces along the deformation zone suggest that bonding will occur along the entire length of the rolled product in all cases considered, although the bonding strength will vary in each case.

References

1. Zakharov A.M. Industrial alloys of non-ferrous metals. Phase composition and structural components. Moscow: Metallurgiya, 1980. 255 p. (In Russ.).
Захаров А.М. Промышленные сплавы цветных металлов. Фазовый состав и структурные составляющие. М.: Металлургия, 1980. 255 с.
2. Belov N.A., Alabin A.N., Matveeva I.A. Optimization of phase composition of Al—Cu—Mn—Zr—Sc alloys for rolled products without requirement for solution treatment and quenching. *Journal of Alloys and Compounds*. 2014;583:206—213. https://doi.org/10.1016/j.jallcom.2013.08.202
3. Belov N.A., Akopyan T.K., Shurkin P.K., Korotkova N.O. Comparative analysis of structure evolution and thermal stability of commercial AA2219 and model Al—2 wt.%Mn—2 wt.%Cu cold rolled alloys. *Journal of Alloys and Compounds*. 2021;864:158823. https://doi.org/10.1016/j.jallcom.2021.158823
4. Ghali E. Corrosion resistance of aluminum and magnesium alloys: Understanding, performance, and testing. Hoboken: John Wiley & Sons, Inc., 2010. 752 p.
5. Zarapin Yu.L., Chichenev N.A., Chernilevskaya N.G. Production of composite materials by forming. Recent achievements. Moscow: Metallurgiya, 1991. 351 p. (In Russ.).
Зарапин Ю.Л., Чиченев Н.А., Чернилевская Н.Г. Производство композиционных материалов обработкой давлением. Последние достижения. М.: Металлургия, 1991. 351 с.
6. Zinoviev A.V., Kolpashnikov A.I., Polukhin P.I., Glebov Yu.P., Piryazev D.I., Gorokhov V.S., Galkin A.M. Technology of forming of non-ferrous metals and alloys: Textbook for universities. Moscow: Metallurgiya, 1992. 512 p. (In Russ.).
Зиновьев А.В., Колпашников А.И., Полухин П.И., Глебов Ю.П., Пирязев Д.И., Горохов В.С., Галкин А.М. Технология обработки давлением цветных металлов и сплавов: Учебник для вузов. М.: Металлургия, 1992. 512 с.
7. Khan H.A., Asim K., Akram F., Hameed A., Khan A., Mansoor B. Roll bonding processes: State-of-the-Art and future perspectives. *Metals*. 2021;11:1344. https://doi.org/10.3390/met11091344
8. Li Z., Rezaei S., Wang T., Han J., Shu X., Pater Z., Huang Q. Recent advances and trends in roll bonding process and bonding model: A review. *Chinese Journal of Aeronautics*. 2023;36(4):36—74. https://doi.org/10.1016/j.cja.2022.07.004
9. Kobelev A.G., Lysak V.I., Chernyshev V.N., Kuznetsov E.V. Materials Science and Technology of Composite Materials. Moscow: Intermet Engineering, 2006. 368 p. (In Russ.).
Кобелев А.Г., Лысак В.И., Чернышев В.Н., Кузнецов Е.В. Материаловедение и технология композиционных материалов: Учебник для вузов. М.: Интермет Инжиниринг, 2006. 368 с.
10. Shatalov R.L., Kulikov M.A. Influence of outer parts of a strip on the deformation and force parameters of thin-sheet rolling. *Metallurgist*. 2020;64:687—698. https://doi.org/10.1007/s11015-020-01045-1
11. Shatalov R.L., Maksimov E.A. Development and application of the theory of rigid ends in thin-sheet rolling. *Metallurgist*. 2021;64:1035—1042. https://doi.org/10.1007/s11015-021-01084-2
12. Rao K.P., Doraivelu S.M., Gopinathan V. Flow curves and deformation of materials at different temperatures and strain rates. *Journal of Mechanical Working Technology*. 1982;6(1):63—88. https://doi.org/10.1016/0378-3804(82)90020-1
13. Polukhin P.I., Gun G.Y., Galkin A.M. Resistance to plastic deformation of metals and alloys. Handbook. Moscow: Metallurgiya, 1983. 352 p. (In Russ.).
Полухин П.И., Гун Г.Я., Галкин А.М. Сопротивление пластической деформации металлов и сплавов: Справочник. М.: Металлургия, 1983. 352 с.
14. Aksöz S., Ocak Y., Maraşlı N., Çadirli E., Kaya H., Böyük U. Dependency of the thermal and electrical conductivity on the temperature and composition of Cu in the Al based Al—Cu alloys. *Experimental Thermal and Fluid Science*. 2010;34(8):1507—1516. https://doi.org/10.1016/j.expthermflusci.2010.07.015
15. Zinoviev V.E. Thermophysical properties of metals at high temperatures: Handbook. Moscow: Metallurgiya, 1989. 384 p. (In Russ.).
Зиновьев В.Е. Теплофизические свойства металлов при высоких температурах: Справочник. М.: Металлургия, 1989. 384 с.
16. QForm. Version 10.3. Windows. Moscow: LLC "Kvantoform", 2023.
QForm. Версия 10.3. Windows. М.: ООО «Квантор-форм», 2023.
17. Vlasov A.V., Stebunov S.A., Evsyukov S.A., Biba N.V., Shitikov A.A. Finite-element modeling of technological processes of forging and stamping: textbook. Moscow: Bauman Moscow State Technical University, 2019. 383 p. (In Russ.).

Власов А.В., Стебунов С.А., Евсюков С.А., Биба Н.В., Шитиков А.А. Конечно-элементное моделирование технологических процессов ковки и объемной штамповки: Учеб. пособие. М.: Изд-во МГТУ им. Н.Э. Баумана, 2019. 383 с.

18. Qin Q., Zhang D., Zang Y., Guan B. A simulation study on the multi-pass rolling bond of 316L/Q345R stainless clad plate. *Advances in Mechanical Engineering*. 2015;7(7). https://doi.org/10.1177/1687814015594313
19. He Z., Chu Z., Shuang Y., Gou Y. The Bonding mechanism and experimental verification of pilger hot rolling clad tube. *Advances in Materials Science and Engineering*. 2020;2020:2689370. https://doi.org/10.1155/2020/2689370
20. Kolpashnikov A.I. Rolling of light alloy sheets. Moscow: Metallurgiya, 1970. 232 p. (In Russ.).
Колпашников А.И. Прокатка листов из легких сплавов. М.: Металлургия, 1970. 232 с.
21. Tselikov A.I., Nikitin G.S., Rokotyan S.E. Theory of flat rolling. Textbook for students of machine-building and metallurgical universities. Moscow: Metallurgiya, 1980. 320 p. (In Russ.).
Целиков А.И., Никитин Г.С., Рокотян С.Е. Теория продольной прокатки: Учебник для студентов машиностроительных и металлургических вузов. М.: Металлургия, 1980. 320 с.
22. Polukhin P.I., Zinoviev A.V., Polukhin V.P., Burov A.V., Shevelkin S.D. Improving the quality of strips from nonferrous metals and alloys. Alma-Ata: Nauka, 1982. 288 p. (In Russ.).
Полухин П.И., Зиновьев А.В., Полухин В.П., Буров А.В., Шевелкин С.Д. Повышение качества полос из цветных металлов и сплавов. Алма-Ата: Наука, 1982. 288 с.
23. Kovalev S.I., Koryagin N.I., Shirkov I.V. Stresses and strains in flat rolling. Moscow: Metallurgiya, 1982. 256 p. (In Russ.).
Ковалев С.И., Корягин Н.И., Ширков И.В. Напряжения и деформации при плоской прокатке. М.: Металлургия, 1982. 256 с.
24. Kebriaei R., Vladimirov I.N., Reese S. Joining of the alloys AA1050 and AA5754 — Experimental characterization and multiscale modeling based on a cohesive zone element technique. *Journal of Materials Processing Technology*. 2014;214(10):2146—2155. https://doi.org/10.1016/j.jmatprotec.2014.03.014
25. Bambach M., Pietryga M., Mikloweit A., Hirt G. A finite element framework for the evolution of bond strength in joining-by-forming processes. *Journal of Materials Processing Technology*. 2014;214(10):2156—2168. https://doi.org/10.1016/j.jmatprotec.2014.03.015
26. Frolov Y., Nosko M., Samsonenko A., Bobukh O., Remez O. Roll bonding of Al-based composite reinforced with C10 steel expanded mesh inlay. *Metals*. 2021;11:1044. https://doi.org/10.3390/met11071044
27. Frolov Y., Bobukh O., Samsonenko A., Nürnberger F. Patterning of surfaces for subsequent roll bonding in a low-oxygen environment using deformable mesh inlays. *Journal of Manufacturing and Materials Processing*. 2023;7:158. https://doi.org/10.3390/jmmp7050158
28. Salikhyanov D.R. Investigation of the stress-strain state at the boundary between materials during rolling of a layered composite. *Chernye Metally*. 2023;9:34—39.
Салихянов Д.Р. Исследование напряженно-деформированного состояния на границе между материалами при прокатке слоистого композита. *Черные металлы*. 2023;9:34—39. https://doi.org/10.17580/chm.2023.09.06
29. Salikhyanov D., Michurov N. Joining of dissimilar aluminum alloys AA5154 and AA2024 by cold roll bonding. *The International Journal of Advanced Manufacturing Technology*. 2023;129:255—277. https://doi.org/10.1007/s00170-023-12292-2

Information about the authors

Aleksander N. Koshmin – Cand. Sci. (Eng.), Associate Professor of Scientific Activity Sector of Moscow Polytechnic University; Associate Professor of Metal Forming Department of National University of Science and Technology "MISIS" (NUST MISIS).
https://orcid.org/0000-0002-4095-1658
E-mail: koshmin.an@misis.ru

Aleksander V. Zinoviev – Dr. Sci. (Eng.), Professor, Senior Expert of Metal Forming Department, NUST MISIS.
https://orcid.org/0009-0004-6776-7414
E-mail: zinovyew@gmail.com

Stanislav O. Cherkasov – Engineer of Metal Forming Department, NUST MISIS.
https://orcid.org/0000-0001-5248-501X
E-mail: cherkasov.so@misis.ru

Kirill A. Tsydenov – Engineer of Metal Forming Department, NUST MISIS.
https://orcid.org/0000-0002-9290-4925
E-mail: kirillcydenov@yandex.ru

Информация об авторах

Александр Николаевич Кошмин – к.т.н., доцент сектора научной деятельности Московского политехнического университета; доцент кафедры обработки металлов давлением Национального исследовательского технологического университета «МИСИС» (НИТУ МИСИС).
https://orcid.org/0000-0002-4095-1658
E-mail: koshmin.an@misis.ru

Александр Васильевич Зиновьев – д.т.н., проф., вед. эксперт научного проекта кафедры обработки металлов давлением, НИТУ МИСИС.
https://orcid.org/0009-0004-6776-7414
E-mail: zinovyew@gmail.com

Станислав Олегович Черкасов – инженер научного проекта кафедры обработки металлов давлением, НИТУ МИСИС.
https://orcid.org/0000-0001-5248-501X
E-mail: cherkasov.so@misis.ru

Кирилл Андреевич Цыденов – инженер научного проекта кафедры обработки металлов давлением, НИТУ МИСИС.
https://orcid.org/0000-0002-9290-4925
E-mail: kirillcydenov@yandex.ru

Contribution of the authors

A.N. Koshmin – manuscript writing, methodology.

A.V. Zinoviev – conceptualization, manuscript review.

S.O. Cherkasov – simulation, results processing.

K.A. Tsydenov – experiment, results discussion.

Вклад авторов

А.Н. Кошмин – написание статьи, методология.

А.В. Зиновьев – концептуализация, рецензирование статьи.

С.О. Черкасов – моделирование, обработка результатов.

К.А. Цыденов – эксперимент, обсуждение результатов.

The article was submitted 12.02.2024, revised 18.04.2024, accepted for publication 25.04.2024

Статья поступила в редакцию 12.02.2024, доработана 18.04.2024, подписана в печать 25.04.2024